Space-resolved electron density and temperature measurements of line-shaped laser plasmas

Ling-qing Zhang, Shen-sheng Han, Zhi-zhan Xu, Zheng-quan Zhang, Pin-zhong Fan, and Lan Sun
Shanghai Institute of Optics and Fine Mechanics, P.O. Box 800-211, Shanghai 201800, People's Republic of China
(Received 14 July 1994; revised manuscript received 9 January 1995)

Line-shaped magnesium laser plasmas were studied using a pinhole crystal spectrograph in our recent work [L. Q. Zhang *et al.*, Nucl. Fusion Plasma Phys. **14**, 55 (1994) (in Chinese)]. Electron density and temperature profiles were obtained using the spectral diagnostic method. Electron densities beyond the critical density were measured when a unique density diagnostic method of Stark-broadened Ly-α line wings was used. A fitting program has been developed. Time-integrated properties of laser plasmas were also discussed and compared with those of spot-shaped laser plasmas and theoretical estimations of a laser absorption model. The conclusion is that the dynamic behaviors of line- and spot-shaped laser plasmas are different.

PACS number(s): 52.25.−b, 33.20.Rm, 52.70.−m, 52.25.Jm

I. INTRODUCTION

It is very important to study the properties of line-shaped laser plasmas as they are widely used as x-ray lasing mediums. Previous studies of such plasmas are mainly about the uniformity of the plasmas in the axial direction [1,2], and plasma parameters deduced from spectra obtained from this direction usually suffer from large opacity and refraction effects, so the accuracy is somewhat unsatisfactory. As for the distribution of plasma parameters in the normal direction, which is more important to x-ray laser research, however, few experimental studies have been conducted because of the difficulty of overcoming source broadening [3]. Apart from simulations of various models, experimental studies of x-ray lasing medium were usually conducted with spot-shaped laser plasmas [4] with the risk of different hydrodynamic behaviors of these two types of laser plasmas. In our recent work, with the help of a pinhole crystal spectrograph (PCS) [3], line-shaped laser plasmas were fully investigated. The space-resolved plasma parameters of the electron density and the temperature were measured in the direction perpendicular to the target surface. Electron densities beyond the critical density were also obtained using the diagnostic method of Stark-broadened Ly-α line wings [5]. Time-integrated properties of line- and spot-shaped laser plasmas were compared and they seem quite different from our study.

II. DETERMINATION OF PROFILES OF ELECTRON TEMPERATURE AND DENSITY

A computer code ESDAP [6] was used in the spectral data processing to obtain the parameter profiles of line-shaped Mg laser plasmas. The profile of the electron temperature was determined from the ratio of the intensity of the dielectronic satellite j to the resonance line intensity of Mg XII ions [7].

The profiles of the electron density were determined by two diagnostic methods: (i) from the ratio of the intensities of the resonance and intercombination lines of He-like ions [8] and (ii) from fitting Stark-broadened line wings of the resonance line $2p$-$1s$ [5]. The Stark-broadened line wings are necessarily optically thin and the density can be deduced directly since the broadening depends only on the ion-produced electric microfield. Theoretical variations of wing intensity with changes in density are investigated in order to demonstrate the sensitivity of the method. A program was developed through which electron density can be obtained by fitting experimental data to theoretical line-wing profiles using a nonlinear least-squares method. This program, unlike that in Ref. [5], can avoid the normalization of the observed profiles by reference to the intensity of the free-bound continuum at the series limit.

Taking into account the effects of Debye screening and radiator-perturber correlations, the theoretical profiles can be calculated from [5]

$$D(\Delta\lambda)=N_n A_{n1}\frac{h\Delta\lambda}{4\pi}L(\Delta\lambda)d\Delta\lambda G(\Delta\lambda)\ , \tag{1}$$

where $G(\Delta\lambda)$ is the response function of the whole detection system, which can be derived by experimental calibration. In a small interval of frequency, $G(\Delta\lambda)$ is approximately a constant, N_n is the number density in the upper state, and A_{n1} is the radiation rate. $L(\Delta\lambda)$ is the line-shape function

$$L(\Delta\lambda)=\frac{k}{CE_0}\omega(\beta)\ , \tag{2}$$

where

$$\omega(\beta)=3x^4\exp\left[-\frac{(Z-1)a'^2}{3x}\exp[-(1+Z_p)^{1/2}a'x]\right]\times\left[a'\left[2+\frac{2}{a'x}+a'x\right]\exp(-a'x)\right]^{-1}\ , \tag{3}$$

$$a'=\frac{r_p}{\lambda_D}\ , \tag{4}$$

$$r_p=\left[\frac{1}{\frac{4}{3}\pi N_p}\right]^{1/3},\quad \lambda_D=\left[\frac{kT_e}{4\pi N_e e^2}\right]^{1/2}, \tag{5}$$

$$E_0=\frac{Z_p e}{r_p^2}\ , \tag{6}$$

$$E=\frac{Z_p e}{r^2}\left[1+\frac{r}{\lambda_D}\right]\exp(-r/\lambda_D)\ , \tag{7}$$

$$\beta=\frac{1}{x^2}[1+a'x]\exp(-a'x)\ , \tag{8}$$

with $\omega(\beta)$ the probability distribution of the ion microfield strength and E a screened field. Values of C, with suitable Z scaling, are given in Ref. [9]. k is a normalization constant such that $\int L(\Delta\lambda)d\Delta\lambda=1$; a' is a screening parameter; $x=r/r_p$; λ_D is the Debye screening length; and r_p, Z_p, and N_p are the averaged separation, the charge, and the number density of the ions of the plasma, respectively.

When β is at small values, it is necessary to restrict the values of a' and Z to ensure that only a small correction may be brought about by Z_p and a'. That is, a' and Z should be within the parameter regime

$$(Z-2)a'^2\leq 0.3\ . \tag{9}$$

Substituting Eqs. (2) and (3) into Eq. (1) and considering $\Delta\lambda=CE$ and $\beta=\Delta\lambda/CE_0$, giving the fitting function of Stark-broadened line wings

$$D(\Delta\lambda)=C'\frac{\Delta\lambda}{CE_0}\omega\left[\frac{\Delta\lambda}{CE_0}\right]\ , \tag{10}$$

then E_0 can be obtained by fitting of experimental data to Eq. (10) using a nonlinear least-squares algorithm:

$$E_0=\left[\frac{4\pi}{3}\right]^{2/3} e\left[\sum Z_p^{3/2}N_p\right]^{2/3}\ , \tag{11}$$

$$N_e=\sum Z_p N_p=Z_{\text{eff}}N_i\ , \tag{12}$$

so N_e can be derived when the population of the various ionization stages is known.

The theoretical intensities of the Ly-α line wings with different N_e were investigated and the results are shown in Fig. 1. It is obvious that they are more sensitive to higher densities, so the density determined at one point by this method corresponds to the highest density of the local plasma.

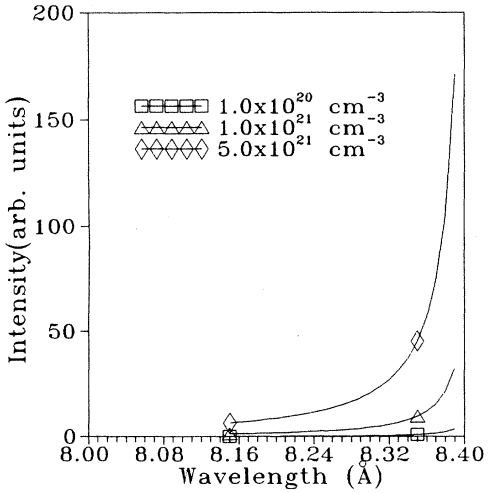

FIG. 1. Variations of the Ly-α line-wing intensity with electron density.

III. EXPERIMENTAL SETUP AND RESULTS

The experiment was carried out at the LF12 Laser Facility of Shanghai Institute of Optics and Fine Mechanics. An aspherical lens ($f/1.7$) was combined with a cylindrical lens array to form a 12 mm$\times$120 μm uniform focal line (the nonuniformity of laser illumination along the focal line is within 5%) on the Mg-slab target surface. In the experiment 600- and 200-J laser beams of 1.05 μm full width at half maximum of 900 ps were used in order to investigate the density profiles as a function of the distance perpendicular to the target surface under different laser fluxes. The corresponding laser intensities on the target surface were 5.0×10^{13} and 1.7×10^{13} W cm^{-2}, respectively. The space-resolved spectra (7–10 Å) of the line-shaped Mg laser plasmas were taken by a thallium acid phthalate (TAP) PCS [3], which had spectral and space-resolved powers of $\lambda/\Delta\lambda\sim800$ and 50 μm, respectively. The spectra were recorded by the calibrated Shanghai 5F x-ray film.

Shown in Fig. 2 are the line wings of Ly-α lines and their fitting curves ($a'=0.1$ in the fitting program) with laser intensities of 600 and 200 J, respectively. The electron density profiles are shown in Fig. 3, where the squares were obtained from the ratio of the intensities of the resonance and the intercombination lines (I_R/I_I). The disagreement of the N_e values with these two diagnostic methods is obvious. The disagreement is mainly due to two aspects: (a) the opacity effect, wherein N_e obtained from I_R/I_I gives an underestimated value near the target surface and becomes more accurate when the distance increases in the normal direction of the target [8] (wings of the Ly-α line, as described in Sec. II, are optically thin), and (b) different diagnostic methods. The density obtained from I_R/I_I represents the averaged N_e of the plasma, while that from the Ly-α line wing corresponds to the highest N_e (see Fig. 1). So the values of data from the Ly-α line wing are higher than those from I_R/I_I. It is worth noting that the data from these two methods agree to some extent when the distance is 300 μm beyond the target surface, as shown in Fig. 3(a).

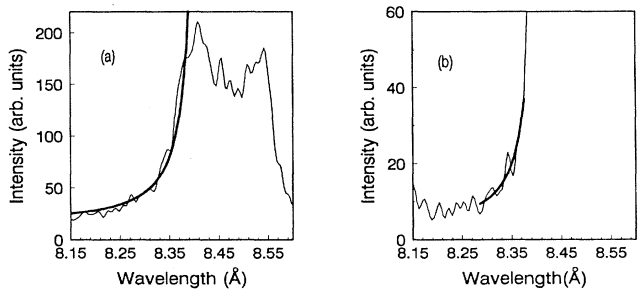

FIG. 2. Line wings of Ly-α of Mg XII and their fitting curves (a) 600J and (b) 200J.

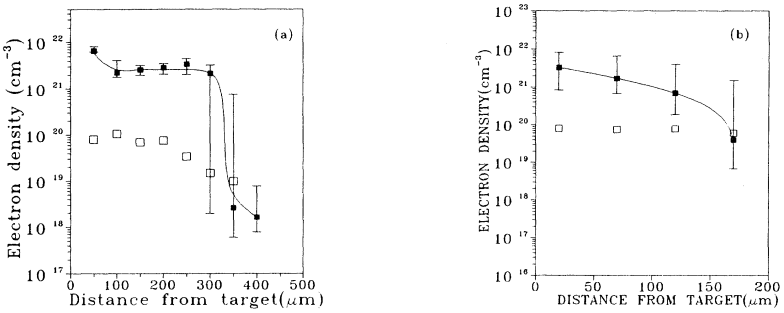

FIG. 3. Electron density profiles perpendicular to the target surface: (a) 600J and (b) 200J [where the squares were obtained by I_R/I_I of Mg XI ($1s^2-1s2p$)].

Three considerations have been taken into account in the data processing when fitting Stark-broadened line wings: (i) The fitting region should vary with the distance from the target in order to make each position have the same error, as E increases with larger N_e near the target surface; (ii) the line wings should be presmoothed as the noise is overlapped in the spectrum; and (iii) taking account of the uncertainty of the line center position in calibrations, a half-width at half maximum of the $2p$-$1s$ line was added in the fitting region, so an error bar is obtained in each space-resolved distance from the target surface (as shown in Fig. 3). Figure 4 shows the time-integrated temperature profile of the Mg laser plasma under a laser irradiation intensity of 600 J.

IV. COMPARISON WITH SPOT-SHAPED LASER PLASMAS

The time-integrated electron thermal pressure profiles obtained in different experiments using the same target and diagnostic methods [10,8] are shown in Fig. 5. The ratios of T_e/T_e' and $P_{\rm th}/P_{\rm th}'$ ($P_{\rm th}=N_eT_e$) for the same kind of target and pumping laser but different irradiation intensity $I(I')$ and pulse length $\tau(\tau')$ can be estimated from [11]

$$\frac{T_e}{T_e'}=\left[\frac{I}{I'}\right]^{1/2}\left[\frac{\tau}{\tau'}\right]^{1/4},\quad \frac{P_{\rm th}}{P_{\rm th}'}=\left[\frac{I}{I'}\right]^{3/4}\left[\frac{\tau}{\tau'}\right]^{-1/8}.$$

Here we neglected the difference between the effective charges Z and Z'. In Table I we present the theoretically and the experimental values of the ratio of electron temperature and thermal electron pressure for the three experiments shown in Fig. 5.

With the assumption that the space-averaged $\langle T\rangle$ and $\langle P\rangle$ are linearly proportional to T_e and $P_{\rm th}$, the agreement of the experimental data with the theoretically estimated values for two spot-shaped laser plasmas is satisfactory. However, for $\langle T_2\rangle,\langle P_2\rangle$ and $\langle T_3\rangle,\langle P_3\rangle$, which correspond to a spot-shaped and a line-shaped laser plasma, respectively, the deviation of the experimental data from the theoretical estimation is remarkable. Because the difference of light absorption between a planar expansion and a spherical expansion can be negligible [11], the time-integrated electron temperature and

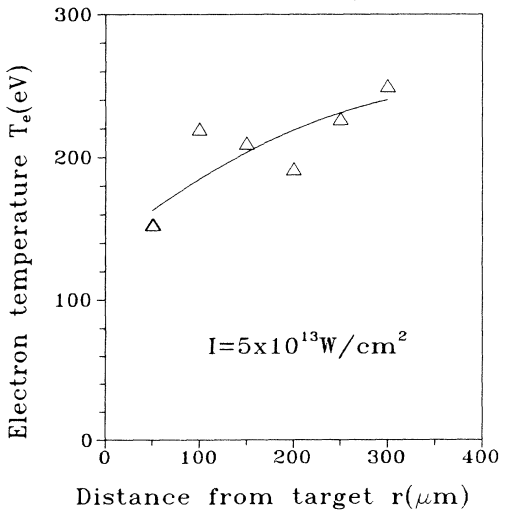

FIG. 4. Electron temperature profiles obtained by I_S/I_R of the Mg XII ion.

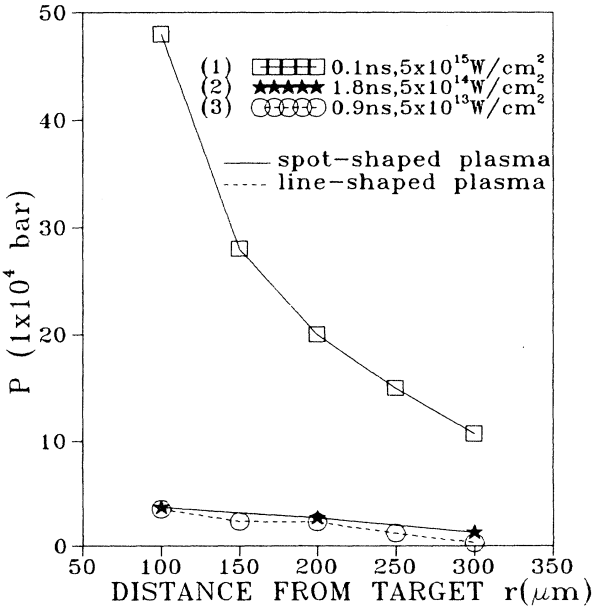

FIG. 5. Time-integrated electron thermal pressure profiles obtained in previous and our experiments using the same diagnostic methods (I_R/I_I). The spot diameter is (1) 100 μm, (2) 80 μm, and (3) 120 μm.

TABLE I. Theoretical and experimental ratios of electron temperatures and thermal electron pressures for the three experimental data shown in Fig. 5.

Ratio	Expt.	Theor.
$\langle T_1 \rangle / \langle T_2 \rangle$	1.53	1.54
$\langle T_2 \rangle / \langle T_3 \rangle$	1.17	3.76
$\langle P_1 \rangle / \langle P_2 \rangle$	9.5	8.1
$\langle P_2 \rangle / \langle P_3 \rangle$	1.3	5.2

the thermal electron pressure in line-shaped laser plasmas are higher than those in the spot-shaped laser plasmas, obviously indicating a different plasma fluid dynamic behavior due to different expansion dimensions.

V. SUMMARY

Properties of line-shaped magnesium laser plasmas along the normal direction of the target surface were investigated with the help of a pinhole crystal spectrograph. Parameter distributions of electron density and temperature were obtained. A spectral diagnostic method of Stark-broadened line wings plus a pinhole crystal spectrograph was applied to line-shaped laser plasmas and obtained densities near the target higher than the critical density. Time-integrated properties of a line-shaped laser plasma were also discussed and compared with those of a spot-shaped laser plasma; the dynamic behaviors of line- and spot-shaped laser plasmas are obviously different.

ACKNOWLEDGMENTS

The authors gratefully acknowledge the LF12 Laser Facility Operation Group for their efforts and Dr. Wei Yu for helpful discussions. This work was supported by the National High Technology Program of China.

[1] M. Nantal *et al.*, in *Proceedings of the 3rd International Colloquium on X-ray Lasers, 1992,* edited by E. E. Fill, IOP Conf. Proc. No. 125 (Institute of Physics and Physical Society, London, 1992), Sec. 7, p. 353.
[2] G. Jamelot *et al.*, in *Proceedings of the 3rd International Colloquium on X-ray Lasers, 1992* (Ref. [1]), Sec. 2, p. 89.
[3] S. S. Han *et al.*, in *Proceedings of the 3rd International Colloquium on X-ray Lasers, 1992* (Ref. [1]), Sec. 7, p. 383.
[4] W. H. Goldstein, *et al.*, Phys. Rev. Lett. **58**, 2300 (1987).
[5] C. C. Smith and N. J. Peacock, J. Phys. B **11**, 2749 (1978).
[6] L. Q. Zhang *et al.*, Acta Opt. Sin. **14**, 785 (1994).
[7] E. V. Aglitskii *et al.*, Kvant. Elektron. (Moscow) **1**, 579 (1974) [Sov. J. Quantum Electron. **4**, 322 (1974)].
[8] V. A. Boiko, S. A. Pikuz, and A. Ya. Faenov, J. Phys. B **12**, 1889 (1979).
[9] H. R. Griem, *Spectral Line Broadening by Plasma* (Academic, New York, 1974), p. 313.
[10] V. I. Bayanov *et al.*, Kvant. Elektron. (Moscow) **3**, 2253 (1976) [Sov. J. Quantum Electron. **6**, 1226 (1976)].
[11] Patrick Mora, Phys. Fluids, **25**, 1051 (1982).